JACC: ADVANCES VOL. 3, NO. 10, 2024

ORIGINAL RESEARCH

AI-Derived Left Ventricular Mass From Noncontrast Cardiac CT

Correlation With Contrast CT Angiography and CMR

Donghee Han, MD,[a,*] Aakash Shanbhag, MSc,[a,b,*] Robert JH. Miller, MD,[a,c] Nicholas Kwok, MD,[a] Parker Waechter, MS,[a] Valerie Builoff, BSc,[a] David E. Newby, MD,[d] Damini Dey, PhD,[a] Daniel S. Berman, MD,[a] Piotr Slomka, PhD[a]

ABSTRACT

BACKGROUND Noncontrast computed tomography (CT) scans are not used for evaluating left ventricle myocardial mass (LV mass), which is typically evaluated with contrast CT or cardiovascular magnetic resonance imaging (CMR).

OBJECTIVES The purpose of the study was to assess the feasibility of LV mass estimation from standard, ECG-gated, noncontrast CT using an artificial intelligence (AI) approach and compare it with coronary CT angiography (CTA) and CMR.

METHODS We enrolled consecutive patients who underwent coronary CTA, which included noncontrast CT calcium scanning and contrast CTA, and CMR. The median interval between coronary CTA and CMR was 22 days (interquartile range: 3-76). We utilized a no new UNet AI model that automatically segmented noncontrast CT structures. AI measurement of LV mass was compared to contrast CTA and CMR.

RESULTS A total of 316 patients (age: 57.1 ± 16.7 years, 56% male) were included. The AI segmentation took on average 22 seconds per case. An excellent correlation was observed between AI and contrast CTA LV mass measures ($r = 0.84$, $P < 0.001$), with no significant differences (136.5 ± 55.3 g vs 139.6 ± 56.9 g, $P = 0.133$). Bland-Altman analysis showed minimal bias of 2.9. When compared to CMR, measured LV mass was higher with AI (136.5 ± 55.3 g vs 127.1 ± 53.1 g, $P < 0.001$). There was an excellent correlation between AI and CMR ($r = 0.85$, $P < 0.001$), with a small bias (−9.4). There were no statistical differences between the correlations of LV mass between contrast CTA and CMR or AI and CMR.

CONCLUSIONS The AI-based automated estimation of LV mass from noncontrast CT demonstrated excellent correlations and minimal biases when compared to contrast CTA and CMR. (JACC Adv. 2024;3:101249) © 2024 The Authors. Published by Elsevier on behalf of the American College of Cardiology Foundation. This is an open access article under the CC BY-NC-ND license (http://creativecommons.org/licenses/by-nc-nd/4.0/).

From the [a]Departments of Medicine (Division of Artificial Intelligence in Medicine), Imaging and Biomedical Sciences Cedars-Sinai Medical Center, Los Angeles, California, USA; [b]Signal and Image Processing Institute, Ming Hsieh Department of Electrical and Computer Engineering, University of Southern California, Los Angeles, California, USA; [c]Department of Cardiac Sciences, University of Calgary, Calgary, Alberta, Canada; and the [d]British Heart Foundation Centre for Cardiovascular Science, University of Edinburgh, Edinburgh, United Kingdom. *Drs Han and Shanbhag have contributed equally to this work.

The authors attest they are in compliance with human studies committees and animal welfare regulations of the authors' institutions and Food and Drug Administration guidelines, including patient consent where appropriate. For more information, visit the Author Center.

Manuscript received April 17, 2024; revised manuscript received August 4, 2024, accepted August 13, 2024.

ISSN 2772-963X https://doi.org/10.1016/j.jacadv.2024.101249

ABBREVIATIONS AND ACRONYMS

AI = artificial intelligence

CAC = coronary artery calcium

CAD = coronary artery disease

CMR = cardiac magnetic resonance imaging

CTA = computed tomography angiography

ECG = electrocardiogram

LV mass = left ventricle myocardial mass

nnU-Net = no new UNet

TS = TotalSegmentator

Accurate assessment of left ventricle myocardial mass (LV mass) is crucial for diagnosis and prognostication of various cardiac diseases.[1-4] While echocardiography and cardiac magnetic resonance imaging (CMR) are commonly used for evaluating cardiac structure, contrast cardiac computed tomography (CT) can also provide cardiac structure information.[5-7] With its high spatial resolution and contrast-to-noise signal with contrast administration, contrast-enhanced cardiac CT angiography (CTA) has demonstrated accurate assessment of cardiac chambers and functions.[6]

Noncontrast coronary artery calcium (CAC) CT scanning is a widely used and rapidly growing procedure for assessing the burden of coronary atherosclerosis.[8-10] However, it has not been employed to date for cardiac structural evaluation due to the absence of contrast enhancement. In particular, noncontrast CT has not been employed to date for evaluating LV mass, which is a well-established prognostic indicator for cardiovascular risk.[11,12]

Noncontrast CT scans exhibit similar CT attenuation between the LV myocardium and blood pool, making it challenging to measure LV mass.[13] Recent advancements in artificial intelligence (AI) and deep learning have shown promise in enhancing the identification of inferred anatomy from learned examples that may not be detectable through routine visual evaluation of noncontrast CT alone.[14,15] In this study, we aimed to assess the feasibility of LV mass estimation from standard noncontrast CAC scans using an AI approach and compare it with clinically reported LV mass from contrast CTA and CMR.

METHODS

STUDY POPULATION. We retrospectively assessed consecutive patients who underwent coronary CTA, which included noncontrast CAC scanning and contrast-enhanced CTA, and CMR within a 12-month interscan interval at Cedars-Sinai Medical Center in Los Angeles, California, USA, from January 2015 to May 2023. We excluded cases with significant artifacts in the LV myocardium due to arrhythmia or intracardiac devices (n = 10). The study protocol complied with the Declaration of Helsinki and was approved by the Cedars-Sinai Institutional Review Board. Written informed consent was waived by the institutional review board due to the retrospective nature of the study. To the extent allowed by data sharing agreements and institutional review board protocols, the results and code from this manuscript will be shared upon written request.

CLINICAL DATA. At the time of CTA or CMR scanning, all patients completed a questionnaire regarding clinical symptoms, cardiovascular risk factors, current medications, and previous cardiac interventions. Premature familial coronary artery disease (CAD) history was defined as a primary relative diagnosed for CAD or cardiac event <55 years for male family members or <65 for female family members. Smoking was defined as either currently smoking or having stopped for <1 year. Hypertension, hypercholesterolemia, and diabetes were defined based on self-reported history.

CTA ACQUISITION AND LV MASS EVALUATION. CTA images, including both noncontrast CAC scanning and contract enhanced coronary CTA, were acquired using dual-source CT scanners (Somatom Flash or Force, Siemens Healthineers). Contrast-enhanced coronary CTA images were acquired using the following protocol: Prospective electrocardiogram (ECG) gating at either end systole or mid diastole or helical with dose modulation, with tube voltage (80-120 kVp) and current 300 to 700 mA, and the tube voltage and current were adjusted by experienced radiologic technologists. In preparation for image acquisition, patients were administered 90 to 120 mL of intravenous contrast (Omnipaque or Visipaque, GE Healthcare) at a rate of 4 to 7 mL/s, sublingual nitrates, and intravenous or oral beta-blockers if indicated for prescan heart rate reduction. Images were reconstructed with a slice thickness of 0.6 mm, an increment of 0.5 mm, 250-mm field of view, and 512 × 512 matrix.

The LV mass was measured by experienced cardiologists from contrast-enhanced coronary CTA using a dedicated workstation (Syngo.via, Siemens Healthineers) based on end-systolic or mid-diastolic phase during standard clinical review. The workstation automatically detected the endocardial and epicardial myocardial borders from the axial image stacks, which were then manually edited in axial or short-axis reformatted views by the readers as required. The LV mass volume excluded the papillary muscle.

CMR ACQUISITION AND LV MASS EVALUATION. All CMR scans were performed using a 1.5-T scanner (Avanto, Siemens Healthineers). Retrospectively gated cine steady-state free precession images were obtained in multiple planes, including a stack of short-axis slices with coverage from the LV base to the apex (6-mm slice thickness, 2-mm interslice gap).

To assess LV mass, LV endocardial and epicardial borders at end-diastole were semiautomated

identified on short-axis steady-state free precession images by experienced cardiologists using a workstation (Vitrea, Vital Images Inc). Papillary muscles were excluded from LV mass. All measurements for CTA and CMR were retrieved from the clinical database. As we utilized the current standard approach for LV mass evaluation in CTA and CMR, no additional modifications were made to reduce measurement errors between CTA and CMR.

NONCONTRAST CT ACQUISITION. Noncontrast CT images were acquired as a part of the coronary CTA for CAC assessment, using a scan protocol of prospective ECG triggering at 50% to 80% of the cardiac cycle with 3 mm slice thickness, 120 kVp tube voltage, and automated tube current adjustment based on patient body size. The noncontrast images were acquired during a single cardiac phase in diastole.

All noncontrast CT was reconstructed into matrix size of 512 × 512, 3-mm slice thickness, and using the standard B35f kernel.

AI MYOCARDIAL SEGMENTATION. LV myocardium was segmented from gated noncontrast CT scans, which were acquired for CAC scoring during CTA scanning, using the TotalSegmentator (TS) model developed by Wasserthal et al.[16] TS utilizes a no new-net UNet (nnU-Net) architecture to automatically segment a variety of anatomic structures from images.[17] The nnU-Net model is an ensemble UNet-based implementation that automatically configures all hyperparameters, including preprocessing, network architecture, training, and postprocessing. The automatic joint configuration optimization of fixed, rule-based, and empirical parameter choices without manual intervention and choice of network between 2D and 3D UNet and cascade ensembles generates a versatile, end-to-end, out-of-the-box, state-of-the-art segmentation model. The TS model was previously trained using expert annotations from contrast images, which were transferred to registered noncontrast images. The publicly released training split of the dataset has 620 cases with cardiac annotation including 137 cases with contrast and 483 noncontrast CT. The TS model was trained on datasets with CT images with contrast agent and well-aligned noncontrast CT images available in a subset of cases. During the original TS training, the segmentation was transferred to the noncontrast CT images, and a nnU-Net was trained on images with and without contrast agent—however, without explicit pairing of the images. This training regimen potentially accounts for inconsistencies in the noncontrast CT segmentations in irregular shapes and larger volumes. No further training or fine-tuning was carried out to mitigate any potential biases among different modalities. The entire dicom volume of CT was loaded for inference. No manual corrections were carried out postinference. LV myocardial segmentation for all images used consistent algorithm parameters throughout the study and the same processing steps were followed for each scan. A standard density factor of 1.055 g/mL was used to convert LV myocardial volume to LV mass calculation. We show the software implementation in Supplemental Figure 1.

STATISTICAL ANALYSIS. Data are expressed as mean ± SD for continuous variables. Categorical variables are presented as a number (percentage). Data were analyzed by paired 2-sided t-tests or Wilcoxon matched-pairs signed-rank test as appropriate. Bland-Altman analysis was carried out to compare the LV mass between AI, contrast CTA, and CMR and used to estimate the bias and 95% CIs. Cronbach's alpha analysis was performed to assess internal consistency between measures. We also utilized mixed-effects linear regression models (with subject as a random effect and age and sex as fixed effects) to evaluate the relationship between measures. Spearman's rank-order correlation was used to compare LV mass between AI, contrast CTA, and CMR. Additional subgroup analyses were also performed on the basis of sex and for the patients who were referred for cardiomyopathy evaluation. A 2-sided P value of <0.05 was considered statistically significant. Python (version 3.74) and libraries scikit learn stats [18] and pycompare[19] were used to estimate these metrics. Significance comparison for P values was carried out on STATA (version 17, StataCorp).

RESULTS

BASELINE CHARACTERISTICS. Baseline clinical characteristics of the study patients are shown in Table 1. The mean age was 57.1 ± 16.7 years, and 56% were male. Study patients had a mean body mass index of 26.7 ± 5.6 kg/m^2. Approximately half of the study patients had a history of hypertension (50.3%) or hypercholesterolemia (45.9%). The proportion of patients with prior CAD history was 13.9%. Regarding indication of imaging tests, 139 (44%) patients were undergoing CMR scanning for cardiomyopathy evaluation, and 49 (15.5%) patients and 34 patients (10.8%) were for coronary artery disease evaluation or myocarditis evaluation, respectively.

Table 2 compares the LV mass values obtained from CMR, contrast CTA, and AI from noncontrast CT.

TABLE 1 Baseline Characteristics of the Study Population (N = 316)

Age, y	57.1 ± 16.7
Male	177 (56.0)
Body mass index, kg/m^2	26.7 ± 5.6
Hypertension	159 (50.3)
Diabetes	44 (13.9)
Hypercholesterolemia	145 (45.9)
Current smoking	6 (1.9)
Family history of premature CAD	24 (7.6)
Prior CAD history	44 (13.9)
Imaging test indication (CMR)	
Cardiomyopathy	139 (44.0)
Coronary artery disease	49 (15.5)
Myocarditis	34 (10.8)
Arrhythmia	23 (7.3)
Heart failure	21 (6.6)
Valvular heart disease	11 (3.5)
Pericardial disease	11 (3.5)
Infiltrative disease	10 (3.2)
Others	18 (5.7)

Mean ± SD or number (%).
CAD = coronary artery disease; CMR = cardiac magnetic resonance imaging.

Figures 1 and 2 display correlation plots and Bland-Altman analysis among the three imaging modalities.

CTA vs AI. There was no significant difference in LV mass measures between the AI and contrast CTA (136.5 ± 55.3 g vs 139.6 ± 56.9 g, $P = 0.133$). Further, an excellent correlation was observed between AI and contrast CTA LV mass measures (r = 0.84, $P < 0.001$) (Figure 1). Bland-Altman analysis showed a minimal bias of 2.9 with 95% CI −1.00 to 6.84 and limits of agreement between the methods of 70.1 and −64.3 g (Figure 2).

CMR vs AI. When compared to CMR, measured LV mass was higher with AI (136 ± 55.3 g vs 127.1 ± 53.1 g, $P < 0.001$). There was an excellent correlation between AI and CMR myocardial mass (r = 0.85, $P < 0.001$) (Figure 1). Bland-Altman analysis indicated a small bias (−9.4) toward higher myocardial mass with AI, with 95% CI −12.84 to −5.80 and limits of agreement of 52.6 and −71.3 (Figure 2). The interclass agreement between CMR and AI for consistency was 0.83 with 95% CI 0.792-0.861 and agreement was 0.818 with 95% CI 0.762-0.860.

CMR VS CONTRAST CT AND AI. The correlation between CMR and contrast CT was 0.86, comparable with the correlation coefficient between CMR and AI (r = 0.85, P for difference = 0.32). Bland-Altman analysis also illustrated a similar degree of biases existed in LV mass between CMR vs contrast CT and CMR vs AI (Figure 2).

Cronbach's alpha for LV mass measured on CTA and CMR is 0.934, CMR and AI is 0.907, and CTA and AI is 0.892, indicating a high level of internal consistency between all the measures. The interclass agreement between CMR and contrast CTA for consistency was 0.877 with 95% CI 0.849-0.90 and agreement was 0.856 with 95% CI 0.766-0.905. The interclass agreement between contrast CTA and AI for consistency was 0.805 with 95% CI 0.762-0.841 and agreement was 0.804 with 95% CI 0.760-0.840. Results of the mixed effects regression model are shown in Supplemental Table 1. The beta-coefficient between AI and CT, AI and CMR, and CT and CMR were 0.845, 0.797, and 0.805, respectively.

SUBGROUP ANALYSIS. The LV mass values from CMR, contrast CTA, and AI were compared separately for men and women, as shown in Table 3. The correlations between LV mass from contrast CTA and AI were similar for both men and women, with the correlation coefficient of 0.75 and 0.77. The mean differences were −0.9 for men and 7.8 for women. In both sexes, the LV mass values from contrast CTA and AI were found to be higher compared to CMR (Table 3) (both $P < 0.001$). When we confined the analysis to

TABLE 2 Comparison of LV Mass From CMR, Contrast CT, and Noncontrast CT (AI)

	Contrast CT	AI	Correlation Coefficient	Mean Difference	*P* Value	LOA
LV mass (g)	139.6 ± 56.9	136.5 ± 55.3	0.84 ($P < 0.001$)	2.9 ± 34.3	0.133	−64.3 to 70.1
	CMR	**AI**	**Correlation Coefficient**	**Mean Difference**	***P* Value**	**LOA**
LV mass (g)	127.1 ± 53.1	136.5 ± 55.3	0.85 ($P < 0.001$)	−9.4 ± 31.6	<0.001	−71.3 to 52.6
	CMR	**Contrast CT**	**Correlation Coefficient**	**Mean Difference**	***P* Value**	**LOA**
LV mass (g)	127.1 ± 53.1	139.6 ± 56.9	0.86 ($P < 0.001$)	−12.3 ± 26.9	<0.001	−64.9 to 40.4

AI = artificial intelligence; CMR = cardiac magnetic resonance imaging; CT = computed tomography; CTA = computed tomography angiography; LOA = limit of agreement; LV mass = left ventricle myocardial mass.

FIGURE 1 Correlation of LV Mass Between CMR, Contrast CT, and AI

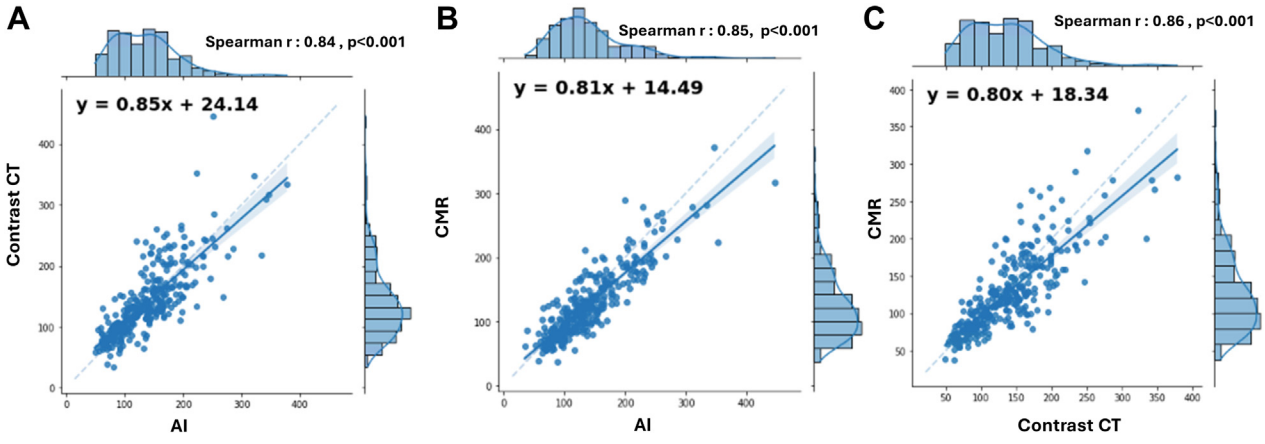

Blue histograms show the distributions of LV mass values in each modality. (A) Contrast CT and AI; (B) cardiac MR (CMR) and AI; (C) cardiac MR (CMR) and contrast CT. AI = artificial intelligence; CMR = cardiac magnetic resonance imaging; CT = computed tomography; LV mass = left ventricle myocardial mass.

patients who underwent CTA and CMR scans specifically for cardiomyopathy evaluation (Table 4), the same trend was observed. The correlation coefficient between contrast CTA and AI was 0.81 with a minimal bias of 4.4. Figure 3 illustrates example cases with CMR, CTA, and LV endocardial and epicardial borders generated from a noncontrast CAC scan using the AI model.

DISCUSSION

In the current study, we evaluated an AI-based method for quantifying LV mass using noncontrast CAC scans. The AI model performed fully automated LV segmentation, with a processing time averaging 22 seconds per case. Our findings demonstrated an excellent correlation and agreement of LV mass between the AI method using noncontrast CT and manual quantification from the contrast CTA (Central Illustration). Moreover, when compared to CMR-derived LV mass, there were no significant differences in the correlation and bias between contrast CTA vs CMR and AI vs CMR. Similar correlations and agreements were observed between women and men and in clinically important subgroup of patients who were referred for cardiomyopathy evaluation. To the

FIGURE 2 Bland-Altman Analysis Between CMR, Contrast CT, and AI

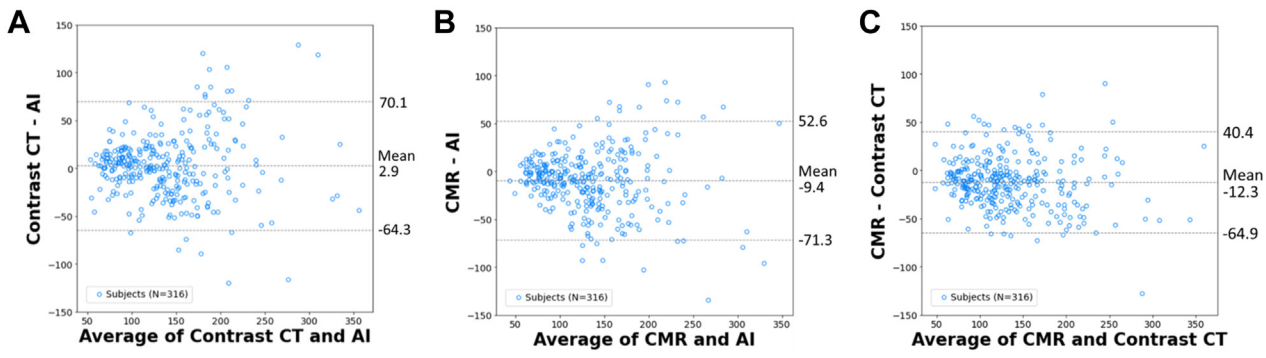

Comparative analysis between different modalities showing mean bias of LV mass (with ±1.96 SD and 95% CIs) as limits of agreement: (A) contrast CT and AI; (B) cardiac MR (CMR) and AI; (C) cardiac MR (CMR) and contrast CT. AI = artificial intelligence; CMR = cardiac magnetic resonance imaging; CT = computed tomography; LV mass = left ventricle myocardial mass.

TABLE 3 Subgroup Analysis: Men and Women

			Men (n = 177)			
	Contrast CT	AI	Correlation Coefficient	Mean Difference	*P* Value	LOA
LV mass (g)	161.0 ± 55.4	161.9 ± 51.6	0.75	−0.9 ± 38.2	0.743	−75.7 to 73.9
	CMR	AI	Correlation Coefficient	Mean Difference	*P* Value	LOA
LV mass (g)	148.9 ± 51.0	161.9 ± 51.6	0.76	−13.1 ± 35.6	<0.001	−82.9 to 56.6
	CMR	Contrast CTA	Correlation Coefficient	Mean Difference	*P* Value	LOA
LV mass (g)	148.9 ± 51.0	161.0 ± 55.4	0.85	−12.1 ± 29.1	<0.001	−69.2 to 44.9
			Women (n = 139)			
	Contrast CT	AI	Correlation Coefficient	Mean Difference	*P* Value	LOA
LV mass (g)	111.9 ± 46.1	104.1 ± 41.2	0.77	7.8 ± 28.1	0.001	−47.1 to 62.7
	CMR	AI	Correlation Coefficient	Mean Difference	*P* Value	LOA
LV mass (g)	99.4 ± 41.6	104.1 ± 41.2	0.78	−4.6 ± 25.1	<0.001	−53.6 to 44.3
	CMR	Contrast CT	Correlation Coefficient	Mean Difference	*P* Value	LOA
LV mass (g)	99.4 ± 41.6	111.9 ± 46.1	0.76	−12.4 ± 23.8	<0.001	−59.0 to 34.1

AI = artificial intelligence; CMR = cardiac magnetic resonance imaging; CT = computed tomography; CTA = computed tomography angiography; LOA = limit of agreement; LV mass = left ventricle myocardial mass.

best of our knowledge, this study is the first to comprehensively validate a fully automated AI-based LV mass evaluation from noncontrast CT by CMR, which is considered the reference standard for LV mass assessment, as well as CTA.

A few recent studies have shown the application of AI algorithms for cardiac chamber segmentation from noncontrast CT.[20,21] However, these studies had limited small sample size and lacked a comparison with the reference standard. For example, Bruns et al developed deep learning algorithm for chamber quantification using dual-energy CT scan data from 18 patients.[21] The algorithm was trained using virtual noncontrast images derived from dual-energy CT data and tested on standard noncontrast CT scans. Although the AI algorithm exhibited reasonable accuracy for segmentation, the quantified chamber volumes and LV mass were lower than those obtained from contrast CTA scans. In our study, we utilized TS, an nnU-Net AI model, which was trained on a subset of 1,204 patients with expert labels transferred from contrast scans onto aligned noncontrast scans.[17] We employed this model to quantify LV mass on ECG-gated noncontrast CAC scans in a relatively large sample size of 316 patients who underwent both coronary CTA and CMR—a reference standard for the clinical evaluation of LV mass. Our findings demonstrated a strong correlation and minimal bias in LV mass quantification between noncontrast CT and both contrast CTA and CMR scans. Importantly, the AI-generated LV mass showed equivalent correlation and biases of LV mass between contrast CTA vs CMR and AI vs CMR.

In this study, we found differences in LV estimation among all three imaging tools. Potential explanations for the discrepancies in myocardial mass

TABLE 4 Subgroup Analysis: Patients Who Referred for Cardiomyopathy Evaluation (n = 139)

			Cardiomyopathy Evaluation (n = 139)			
	Contrast CTA	AI	Correlation Coefficient	Mean Difference	*P* Value	LOA
LV mass (g)	158.1 ± 64.3	153.7 ± 61.7	0.81	4.4 ± 39.6	0.194	−73.2 to 81.9
	CMR	AI	Correlation Coefficient	Mean Difference	*P* Value	LOA
LV mass (g)	144.4 ± 58.7	153.7 ± 61.7	0.81	−9.3 ± 37.4	0.004	−82.6 to 63.9
	CMR	Contrast CT	Correlation Coefficient	Mean Difference	*P* Value	LOA
LV mass (g)	144.4 ± 58.7	158.1 ± 64.3	0.89	−13.7 ± 28.3	<0.001	−69.2 to 41.8

AI = artificial intelligence; CMR = cardiac magnetic resonance imaging; CT = computed tomography; CTA = computed tomography angiography; LOA = limit of agreement; LV mass = left ventricle myocardial mass.

FIGURE 3 Case Examples

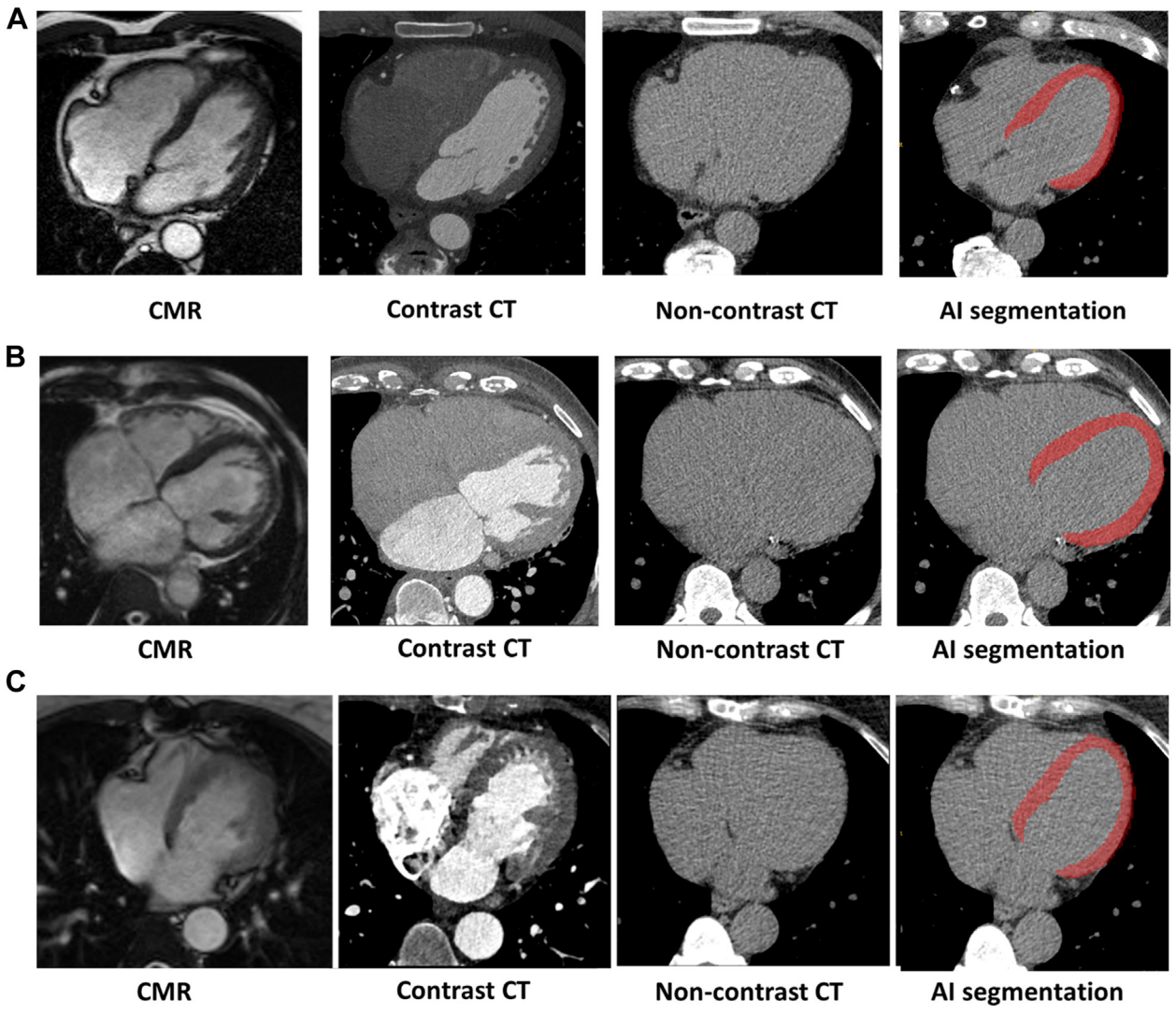

(A) Sixty-five-year-old man presenting with noncardiac chest pain. LV mass by CMR: 130 g, contrast CT: 149 g, AI: 164 g. (B) Seventy-four-year-old man presenting with shortness of breath and with a prior history of coronary revascularization, evaluation for ischemic cardiomyopathy. LV mass by CMR: 205 g; contrast CT: 242 g; and AI: 239 g. (C) Fifty-year-old woman presenting with shortness of breath and with a history of aortic regurgitation, status post-aortic valve surgery 12 years ago. LV mass by CMR: 91 g; contrast CT: 104 g; and AI: 92 g. AI = artificial intelligence; CMR = cardiac magnetic resonance imaging; CT = computed tomography; LV mass = left ventricle myocardial mass.

between modalities include differences in image acquisition methods, contrast-to-noise ratios, and the use of different image stacks (axial vs short-axis images) for the LV mass measurement and reader subjectivity. Other specific reasons include CMR quantification from short-axis slices, which may lead to some truncation of the myocardium in the basal part. Furthermore, CMR can more easily differentiate between the septal wall and the right ventricle compared to CTA, as CTA often has low contrast in right ventricle, making it difficult to distinguish the myocardial border. However, we used standard methods of CTA and CMR for LV mass estimation, which are currently used tools in clinical practice. Our findings highlight the overall high correlation and low bias of LV mass measurement using noncontrast CT scans compared to the two imaging modalities frequently used for clinical purposes in various

CENTRAL ILLUSTRATION **Artificial Intelligence-Based Left Ventricular Mass Quantification for Noncontrast CT**

AI-derived left ventricular mass from noncontrast cardiac CT: correlation with contrast CT angiography and CMR

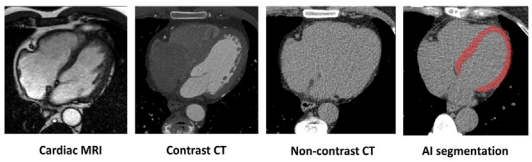

- Retrospective study of 316 patients who underwent non-contrast CT coronary artery calcium (CAC) scan, contrast CT angiography (CTA) and cardiac MRI (CMR).
- An nn-Unet AI model was used for automated LV mass segmentation, with an average processing time of 22 seconds per case.
- The AI-generated LV mass showed equivalent correlation and biases of LV mass between contrast CTA vs. MRI (r=0.86, mean difference: -12.3) and AI vs MRI (r=0.85, mean difference: -9.4).

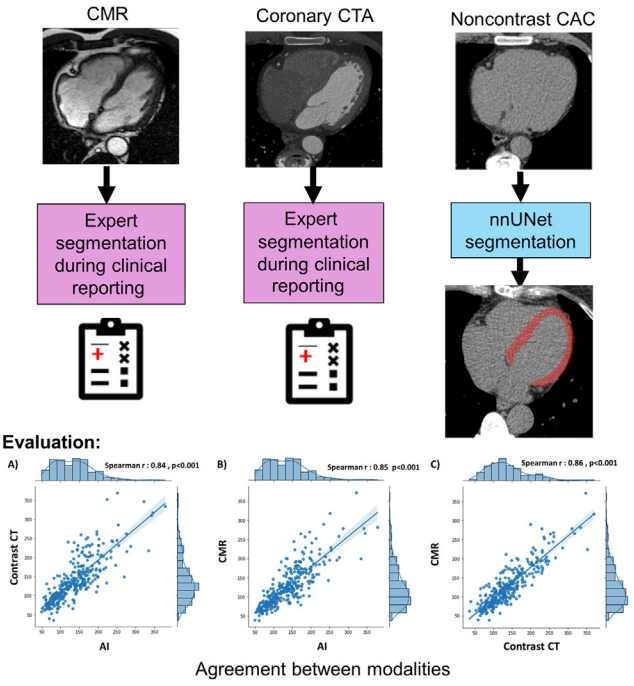

Han D, et al. JACC Adv. 2024;3(10):101249.

The AI-based automated estimation of LV mass from noncontrast CT demonstrates excellent correlations and minimal biases when compared to measurements obtained from contrast CTA and CMR, providing an additional imaging biomarker previously thought not measurable by this modality. AI = artificial intelligence; CMR = cardiac magnetic resonance imaging; CT = computed tomography; CTA = computed tomography angiography; LV mass = left ventricle myocardial mass.

cardiovascular diseases. The image acquisition method, prospective ECG gating vs helical ECG gating, may affect LV mass measurement, though we expect the changes to be minimal.

Although our findings showed a high correlation with overall small bias, Bland-Altman analysis indicated that discrepancies tended to increase with higher LV mass. The most likely reason for this discrepancy is that AI-based models (such as TS) estimate myocardial border and LV cavity size in noncontrast CT images from the training population. In patients with LV mass, the relationship between myocardial wall thickness and ventricular cavity size can diverge.[22,23] Consequently, in cases with larger LV mass and larger cavity, there is a higher likelihood of discrepancies. Additionally, there is clinical variability in reporting CTA and CMR LV mass, as shown in our results, which is another factor for these discrepancies.

In line with the above, AI model may have limitations in LV estimation due to differences in LV shape, size, or focal changes. Therefore, we performed subgroup analyses between men and women, and a group of patients referred for cardiomyopathy evaluation. It is well known that there are distinct differences in LV mass between men and women [24] and certain cardiomyopathy can cause focal LV hypertrophy (hypertrophic cardiomyopathy) or thinning (ischemic cardiomyopathy or dilated cardiomyopathy).[25] Our subgroup analysis demonstrated a comparable high correlation and agreement of LV mass in both sexes and in patients suspected of cardiomyopathies. However, several remaining technical issues may affect the accuracy of the AI model, such as boundary approximation between the right ventricle and septum, errors in approximating septal curvature, differences between catenoid and other LV shapes, variability in cardiac positioning, and various lung and chest wall diseases, as well as postsurgical changes that may alter anatomy. Additional training of the AI algorithm on a wider spectrum of patient

populations will likely improve its accuracy, resulting in broadening the application of AI-based LV mass estimation from noncontrast CT scanning.

An important aspect of LV mass evaluation is its relatively consistent quantification across cardiac cycles.[26] Therefore, unlike cardiac chamber volumes, which heavily depend on the acquisition cardiac phase, LV mass evaluation can be widely applicable to patients undergoing a broad range of CT scans, which include the heart within the field of view and are acquired in just one phase, such as ECG-gated CAC scans.

We found that LV estimation is feasible in ECG-gated noncontrast CAC scans using an AI model. Current guidelines suggest the use of CAC scoring in a broad population of patients with intermediate cardiovascular disease risk.[27] Given the known strong relationship between LV mass and prognosis,[11,28] the LV mass information obtained from CAC scans (without additional radiation, contrast, or special protocols/reconstruction) has high potential for widespread application in patients undergoing CAC scanning. This approach could improve risk stratification and diagnosis, guiding the need for further evaluation in those suspected of having cardiomyopathy who were found to have low or very high myocardial mass from CAC scanning. This technique could potentially be applied to non-ECG gated noncontrast CT scans, which have further broader indications, such as lung cancer screening CT. This may provide cardiovascular disease screening along with CAC scoring in noncontrast nongated CT scans,[29] eventually offering a valuable prognostic imaging biomarker.

STUDY LIMITATIONS. Our study has several limitations. The current study was conducted at a single center utilizing specific CT and CMR scanners, which could limit the generalizability of our findings. We utilized measurements from a single operator for CTA and CMR and, therefore, cannot evaluate the intraobserver variability in these measurements. However, previous studies have shown that the measurements are highly reproducible.[30,31] Our evaluation of the AI model was only with ECG-gated, noncontrast CT scans for CAC scanning. Further studies need to validate the performance of the AI model on non-ECG-gated CT scans. The assessment of LV mass was conducted using varying cardiac phases for each modality. Specifically, noncontrast CT utilized the 50% to 80% phase of the cardiac cycle, contrast CTA employed either end-systole or mid-diastole phases, and quantification of LV mass on CMR was conducted at end-diastole. This discrepancy in the timing of image acquisition has the potential to introduce bias in LV measurements. Nevertheless, a previous study demonstrated that the evaluation of LV mass remained consistent throughout the cardiac cycle.[26] We used the standard approaches to measure LV mass in each modality and then compared it to the new LV mass measurement from noncontrast CT scans, and no efforts were made to minimize systematic errors between any of the approaches. Although our study has a relatively large sample size in this type of study, the limited number of patients and selection bias from including patients who underwent CTA and CMR preclude us from establishing normal reference values. Future work including a cohort of patients with normal LV mass on CTA could be used to establish normal ranges for AI-based LV mass, which could potentially offer clinically valuable information.

CONCLUSIONS

The AI-based automated estimation of LV mass from noncontrast CT demonstrated excellent correlations and minimal biases when compared to measurements obtained from contrast CTA and CMR. This fully automated measure could be applied for routine evaluation of LV mass in patients who have undergone a noncontrast CT scan, providing an additional imaging biomarker previously thought not measurable by this modality.

FUNDING SUPPORT AND AUTHOR DISCLOSURES

This research was supported in part by grant R35HL161195 from the National Heart, Lung, and Blood Institute/National Institutes of Health (NHLBI/NIH) (PI: Piotr Slomka), grant R01EB034586 from the National Institute of Biomedical Imaging and Bioengineering (NIBIB) and a grant from the Dr Miriam and Sheldon G. Adelson Medical Research Foundation. Drs Berman and Slomka participate in software royalties for QPS software at Cedars-Sinai Medical Center. Dr Berman is a consultant for GE Healthcare. Dr Slomka has received research grant support from Siemens Medical System and consulting fees from Synektik, SA. Dr Miller has received research support and consulting fees from Pfizer. Dr Newby is supported by the British Heart Foundation, is a recipient of a Wellcome Trust Senior Investigator Award (WT103782AIA), and has received honoraria for consultancy and lectures from AstraZeneca. The content is solely the responsibility of the authors and does not necessarily represent the official views of the National Institutes of Health. All other authors have reported that they have no relationships relevant to the contents of this paper to disclose.

ADDRESS FOR CORRESPONDENCE: Dr Piotr Slomka, Cedars-Sinai Medical Center, 6500 Wilshire Blvd, Los Angeles, California 90048, USA. E-mail: Piotr.Slomka@cshs.org. X handle: @Piotr_JSlomka.

PERSPECTIVES

COMPETENCY IN MEDICAL KNOWLEDGE: AI-based, fully automated assessment of left ventricle myocardial mass from noncontrast CT scan for calcium score is feasible and showed an excellent correlation and low bias compared with CTA and CMR.

TRANSLATIONAL OUTLOOK 1: Future studies are needed to examine the diagnostic and prognostic utility of the AI-based automated measure of LV mass from a noncontrast CT scan in a variety of cardiac diseases.

TRANSLATIONAL OUTLOOK 2: In the near future, the AI method may be integrated into clinical practice for automatic risk stratification. By providing reliable left ventricular mass measurements, these methods can contribute to more precise and individualized patient risk profiles, aiding in the early detection and management of cardiovascular diseases.

REFERENCES

1. St John Sutton M, Pfeffer MA, Moye L, et al. Cardiovascular death and left ventricular remodeling two years after myocardial infarction: baseline predictors and impact of long-term use of captopril: information from the Survival and Ventricular Enlargement (SAVE) trial. *Circulation*. 1997;96:3294-3299.

2. Vasan RS, Larson MG, Levy D, Evans JC, Benjamin EJ. Distribution and categorization of echocardiographic measurements in relation to reference limits: the Framingham Heart Study: formulation of a height- and sex-specific classification and its prospective validation. *Circulation*. 1997;96:1863-1873.

3. Olivotto I, Maron MS, Autore C, et al. Assessment and significance of left ventricular mass by cardiovascular magnetic resonance in hypertrophic cardiomyopathy. *J Am Coll Cardiol*. 2008;52:559-566.

4. Cikes M, Solomon SD. Beyond ejection fraction: an integrative approach for assessment of cardiac structure and function in heart failure. *Eur Heart J*. 2016;37:1642-1650.

5. Lin FY, Devereux RB, Roman MJ, et al. Cardiac chamber volumes, function, and mass as determined by 64-multidetector row computed tomography: mean values among healthy adults free of hypertension and obesity. *JACC Cardiovasc Imaging*. 2008;1:782-786.

6. Greupner J, Zimmermann E, Grohmann A, et al. Head-to-head comparison of left ventricular function assessment with 64-row computed tomography, biplane left cineventriculography, and both 2- and 3-dimensional transthoracic echocardiography: comparison with magnetic resonance imaging as the reference standard. *J Am Coll Cardiol*. 2012;59:1897-1907.

7. Klein R, Ametepe ES, Yam Y, Dwivedi G, Chow BJ. Cardiac CT assessment of left ventricular mass in mid-diastasis and its prognostic value. *Eur Heart J Cardiovasc Imaging*. 2017;18:95-102.

8. Grundy SM, Stone NJ, Bailey AL, et al. 2018 AHA/ACC/AACVPR/AAPA/ABC/ACPM/ADA/AGS/APhA/ASPC/NLA/PCNA guideline on the management of blood cholesterol: executive summary: a report of the American College of cardiology/American heart association task Force on clinical practice guidelines. *J Am Coll Cardiol*. 2019;73:3168-3209.

9. Budoff MJ, Shaw LJ, Liu ST, et al. Long-term prognosis associated with coronary calcification: observations from a registry of 25,253 patients. *J Am Coll Cardiol*. 2007;49:1860-1870.

10. Kim KP, Einstein AJ, Berrington de González A. Coronary artery calcification screening: estimated radiation dose and cancer risk. *Arch Intern Med*. 2009;169:1188-1194.

11. Levy D, Garrison RJ, Savage DD, Kannel WB, Castelli WP. Prognostic implications of echocardiographically determined left ventricular mass in the Framingham Heart Study. *N Engl J Med*. 1990;322:1561-1566.

12. Schillaci G, Verdecchia P, Porcellati C, Cuccurullo O, Cosco C, Perticone F. Continuous relation between left ventricular mass and cardiovascular risk in essential hypertension. *Hypertension*. 2000;35:580-586.

13. Qanadli SD, Jouannic AM, Dehmeshki J, Lu TL. CT attenuation values of blood and myocardium: rationale for accurate coronary artery calcifications detection with multi-detector CT. *PLoS One*. 2015;10:e0124175.

14. Hosny A, Parmar C, Quackenbush J, Schwartz LH, Aerts H. Artificial intelligence in radiology. *Nat Rev Cancer*. 2018;18:500-510.

15. Singh A, Kwiecinski J, Cadet S, et al. Automated nonlinear registration of coronary PET to CT angiography using pseudo-CT generated from PET with generative adversarial networks. *J Nucl Cardiol*. 2023;30:604-615.

16. Wasserthal J, Breit HC, Meyer MT, et al. TotalSegmentator: robust segmentation of 104 anatomic structures in CT images. *Radiol Artif Intell*. 2023;5:e230024.

17. Isensee F, Jaeger PF, Kohl SAA, Petersen J, Maier-Hein KH. nnU-Net: a self-configuring method for deep learning-based biomedical image segmentation. *Nat Methods*. 2021;18:203-211.

18. Virtanen P, Gommers R, Oliphant TE, et al. SciPy 1.0: fundamental algorithms for scientific computing in Python. *Nat Methods*. 2020;17:261-272.

19. jaketmp LT. *jaketmp/pyCompare: (v1.5.2)*. Zenodo; 2021.

20. Shahzad R, Bos D, Budde RP, et al. Automatic segmentation and quantification of the cardiac structures from non-contrast-enhanced cardiac CT scans. *Phys Med Biol*. 2017;62:3798-3813.

21. Bruns S, Wolterink JM, Takx RAP, et al. Deep learning from dual-energy information for whole-heart segmentation in dual-energy and single-energy non-contrast-enhanced cardiac CT. *Med Phys*. 2020;47:5048-5060.

22. Bluemke DA, Kronmal RA, Lima JA, et al. The relationship of left ventricular mass and geometry to incident cardiovascular events: the MESA (Multi-Ethnic Study of Atherosclerosis) study. *J Am Coll Cardiol*. 2008;52:2148-2155.

23. Miller RJH, Mikami Y, Heydari B, et al. Sex-specific relationships between patterns of ventricular remodelling and clinical outcomes. *Eur Heart J Cardiovasc Imaging*. 2020;21:983-990.

24. Salton CJ, Chuang ML, O'Donnell CJ, et al. Gender differences and normal left ventricular anatomy in an adult population free of hypertension. A cardiovascular magnetic resonance study of the Framingham Heart Study Offspring cohort. *J Am Coll Cardiol*. 2002;39:1055-1060.

25. Juliani PS, Das-Neves-Pereira JC, Monteiro R, Correia AT, Moreira LFP, Jatene FB. Left ventricular chamber geometry in cardiomyopathies: insights from a computerized anatomical study. *ESC Heart Fail*. 2018;5:355-364.

26. Budoff MJ, Ahmadi N, Sarraf G, et al. Determination of left ventricular mass on cardiac computed tomographic angiography. *Acad Radiol*. 2009;16:726-732.

27. Grundy SM, Stone NJ, Bailey AL, et al. 2018 AHA/ACC/AACVPR/AAPA/ABC/ACPM/ADA/AGS/APhA/ASPC/NLA/PCNA guideline on the management of blood cholesterol: a report of the American College of cardiology/American heart association task Force on clinical practice guidelines. *J Am Coll Cardiol*. 2019;73:e285-e350.

28. Kawel-Boehm N, Kronmal R, Eng J, et al. Left ventricular mass at MRI and long-term risk of cardiovascular events: the multi-ethnic study of atherosclerosis (MESA). *Radiology*. 2019;293:107-114.

29. Sandhu AT, Rodriguez F, Ngo S, et al. Incidental coronary artery calcium: opportunistic screening of previous nongated chest computed tomography scans to improve statin rates (NOTIFY-1 project). *Circulation*. 2023;147:703-714.

30. Fieno DS, Jaffe WC, Simonetti OP, Judd RM, Finn JP. TrueFISP: assessment of accuracy for measurement of left ventricular mass in an animal model. *J Magn Reson Imag*. 2002;15:526-531.

31. Schwarz F, Takx R, Schoepf UJ, et al. Reproducibility of left and right ventricular mass measurements with cardiac CT. *J Cardiovasc Comput Tomogr*. 2011;5:317-324.

KEY WORDS artificial intelligence, cardiac magnetic resonance imaging, computed tomography, myocardial mass

APPENDIX For a supplemental table and figure, please see the online version of this paper.